Critical Properties and High-Pressure Volumetric Behavior of the Carbon Dioxide + Propane System at $T = 308.15$ K. Krichevskii Function and Related Thermodynamic Properties

Sofía T. Blanco, Laura Gil, Pilar García-Giménez, Manuela Artal, Santos Otín, and Inmaculada Velasco*

Departamento de Química Orgánica y Química Física, Facultad de Ciencias, Universidad de Zaragoza, 50009-Zaragoza, Spain

Received: January 20, 2009; Revised Manuscript Received: March 19, 2009

Critical properties and volumetric behavior for the $\{CO_2(1) + C_3H_8(2)\}$ system have been studied. The critical locus was measured with a flow apparatus and detected by critical opalescence. For the mixtures, repeatabilities in critical temperature and pressure are $r_{T_c} \leq 0.15$ K and $r_{P_c} \leq 0.013$ MPa, respectively, and the confidence intervals calculated are c.i.$(T_c) < 0.32$ K and c.i.$(P_c) < 0.034$ MPa. The value for the Krichevskii parameter, $A_{Kr} = -4.12$ MPa, was obtained from the experimental critical data in this work. Additionally, the density measurements of 15 $\{CO_2(1) + C_3H_8(2)\}$ binary mixtures at 308.15 K and pressures up to 20 MPa were carried out using an Anton Paar DMA 512-P vibrating-tube densimeter calibrated with the forced path mechanical calibration model. The mean relative standard deviation of density, $\bar{s}^r_\rho$, was estimated to be better than 0.1%, and the uncertainties in temperature and pressure are ±0.01 K and ±0.001 MPa, respectively. In the experimental setup, an uncertainty in the mole fraction, $u(x_j) = \pm 0.0015$, has been achieved. Other properties related to P-ρ−T-x data such as saturated densities, ρ^L and ρ^V, compressibility factor, Z, excess molar volumes, V^E_m, and partial molar volumes, $\bar{V}_i$, have been calculated. Structural properties such as direct and total correlation function integrals and cluster size were calculated using the Krichevskii function concept. Both the critical and volumetric behavior have been compared with literature data and with those obtained from the PC-SAFT and Patel−Teja equations of state.

Introduction

Good quality data of high pressure phase equilibrium (critical points, $P\rho T$, VLE, etc.) for pure compounds and mixtures are important for different industries. For example, it is vital for petroleum and natural gas industries, design of chemical reactors, high pressure extraction and separation equipment, or assessment of processes involving supercritical fluids (SCFs). Furthermore, the capture and storage of CO_2 in geological reservoirs is now considered to be one of the main options for achieving deep reduction in greenhouse gas emissions. The process of capture and storage of CO_2 involves three stages: capture of CO_2 from the power plant or industrial process, transmission of the CO_2 to the storage site and then, storage by injection into the geological reservoir. The availability of data for chemical physical properties such as critical and high pressure volumetric properties of the fluid to be processed becomes indispensable given that the transmission of the fluid is done under supercritical conditions, which takes advantage of the characteristic high volume reduction of the dense phase in comparison with subcritical phases. Moreover, the composition of the fluid, meaning the type, combination, and quantity of impurities, affects the physical and transport properties of CO_2 such as density, compressibility, and so forth, which is a fact that consequently affects pipeline design, compressor power, recompression distance, and pipeline capacity and could also have implications for the prevention of fracture propagation.[1]

The aim of this study is to provide experimental information about the critical and volumetric behavior of the system carbon dioxide plus propane, which depends on the composition of the mixture but also on the P-T region where the state of the mixture studied is found. With this aim in mind, we have measured the critical locus for our system using a flow apparatus based on the critical opalescence phenomenon. Furthermore, densities at low and high pressure, ρ, have been measured using a vibrating tube densimeter for fifteen mixtures with compositions covering the whole range of mole fractions at $T = 308.15$ K and pressures up to 20 MPa. Additionally, we have studied the volumetric behavior of the system in the subcritical region, close to the critical locus and in the supercritical region. Saturated densities, ρ^L and ρ^V, excess molar volumes, V^E_m, and partial molar volumes, $\bar{V}_i$, were derived from experimental densities and were represented by PC-SAFT[2] and Patel−Teja equations of state (PT[3] EoS). This part of our study has been accomplished by determining some structural properties of the $\{CO_2(1) + C_3H_8(2)\}$ system. The isothermal, isochoric derivative of pressure with respect to composition, $(\partial P/\partial x)^\infty_{T,V}$, which is the so-called Krichevskii function, plays an important role in thermodynamics of binary mixtures and reflects to a large degree the mismatch in pure-component equation of state properties. The derivative becomes particularly important for dilute mixtures near the vapor−liquid critical point of the solvent. The value of the derivative at infinite dilution of the solute 2 and the critical point of the solvent 1 has been termed Krichevskii parameter, $A_{Kr} = (\partial P/\partial x)^c_{T_c,V_c}$, and shown[4] to govern the properties of dilute solutions at the conditions of solvent's critical point. Mixtures composed of trace amounts of a solute in the vicinity of a

* To whom correspondence should be addressed. E-mail: curra@unizar.es.

10.1021/jp9005873 CCC: $40.75
Published on Web 04/27/2009

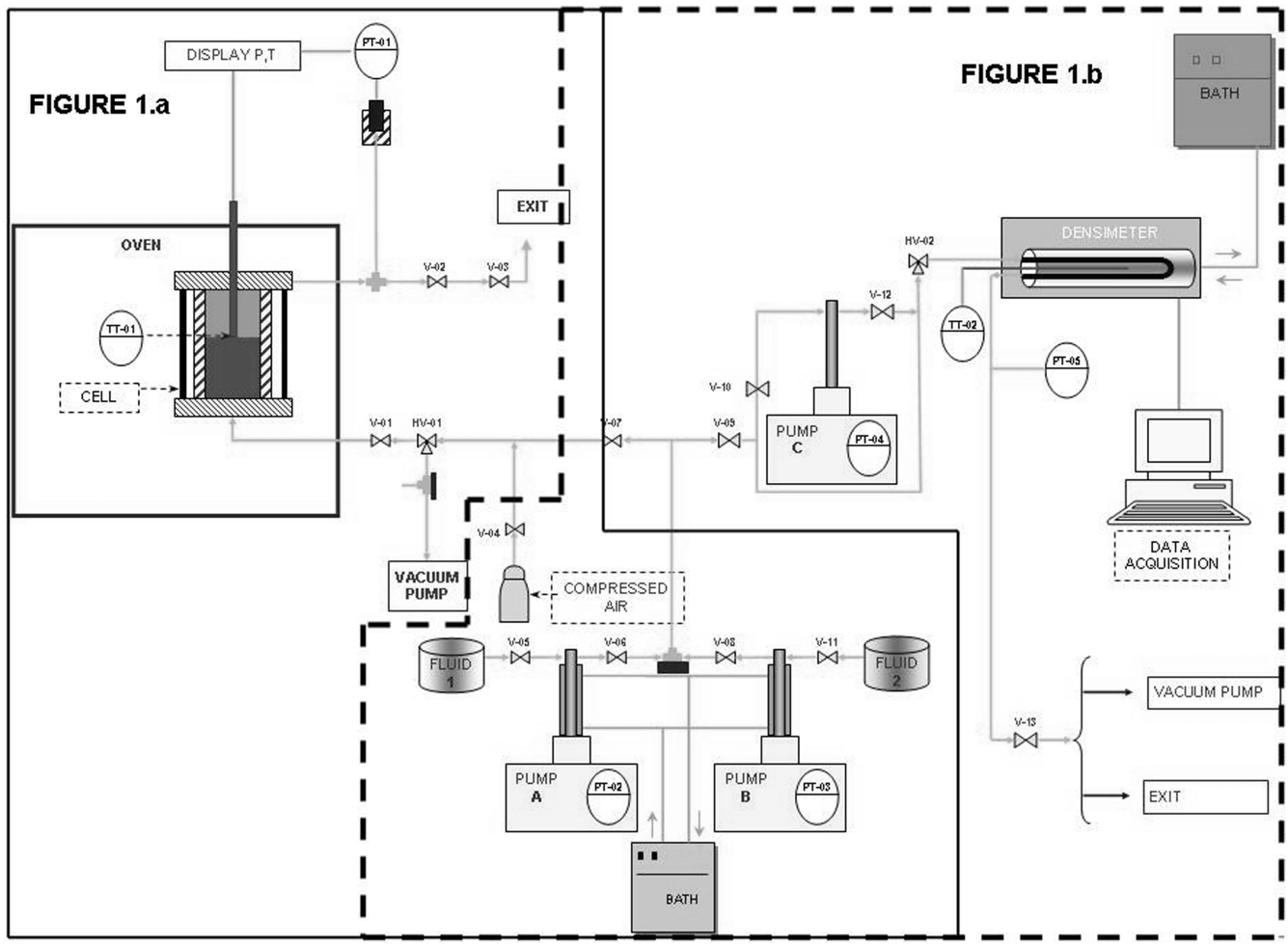

Figure 1. Experimental setup to measure critical properties of pure and binary mixtures (a) and their densities (b): (PT) pressure transducer, (TT) temperature probe, (V) and (HV) valves.

solvent's critical point may exhibit three different types of behavior: repulsive, weakly attractive, or attractive. Each regime is characterized by the signs of the diverging solute partial molar volume and of the correlations between solute and solvent concentration fluctuations at infinite dilution. In this work, we will deduce that our system shows an attractive regime.

There are several data sets in the literature[5–10] of the critical locus for carbon dioxide plus propane system, three sets of high pressure P-ρ-T data,[11–13] and a revision of the saturation data of Reamer et al.[11] by Niesen and Rainwater.[5] Reamer et al.[11] give values of P-V-T for carbon dioxide plus propane mixtures in the vapor−liquid equilibrium, VLE, for vapor and liquid phases separately. We cannot compare our values for density with those for volume from Reamer et al.,[11] given that we cannot measure separately the density of the two phases in equilibrium. Densities of the carbon dioxide plus propane system from Galicia Luna et al.[12] and de la Cruz de Dios et al.,[13] which are measured at temperatures different than 308.15 K, show a good correlation with the densities from our current work. As far as we know, there are no previous data in the literature on excess volumes for this system at the studied range of pressures.

Experimental Section

Materials. Carbon dioxide (mole fraction > 99.98%) and propane (mole fraction > 99.95%) were obtained from Air Liquide.

Apparatus and Procedures. The experimental setup used in this work (Figure 1) is the same as that described in previous studies[14] and consists of two parts that can work independently. Part (a) is a flow apparatus for the determination of critical temperature and pressure (P_c, T_c) of both pure fluids and mixtures. Part (b) is used in the measurement of volumetric properties (P-ρ-T), the main component of which is a vibrating tube density meter.

The loading section, common to parts (a) and (b), consists of two thermostatic chromatography syringe pumps (ISCO, Model 260D) in which the pure substances (liquefied gases) are stored, providing a flow of defined constant composition. The pumps have pressure readers and are cooled with a methanol bath to keep the pressure and temperature of the fluid constant. The uncertainty of the reported mole fraction, $u(x_j)$ was calculated with eq 1 using the rules of propagation of random

TABLE 1: Critical Locus, (P_c, T_c, x_c), for the {CO_2(1) + C_3H_8(2)} Binary System

x_1	P_c/MPa	T_c/K	x_1	P_c/MPa	T_c/K
0.0000	4.253	369.84	0.5549	6.434	330.89
0.0496	4.466	367.51	0.6049	6.532	325.79
0.0949	4.627	365.65	0.6658	6.592	321.58
0.1442	4.914	361.67	0.7227	6.645	316.68
0.1894	5.069	359.59	0.7520	6.686	314.37
0.2567	5.442	353.86	0.8072	6.747	310.05
0.3050	5.623	350.86	0.8454	6.799	307.69
0.3568	5.831	347.14	0.9060	6.961	305.37
0.3956	5.957	344.48	0.9500	7.128	304.59
0.4582	6.156	339.50	1.0000	7.383	304.21
0.5046	6.283	335.90			

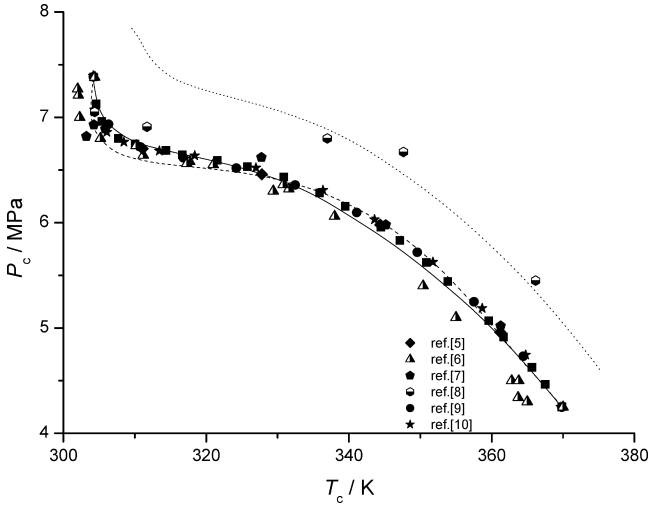

Figure 2. Critical pressure, P_c, versus critical temperature, T_c, for the carbon dioxide plus propane system: (■), experimental results from this work; calculated using PC-SAFT EoS[2] with (—) readjusted and (.....) original parameters; (---), calculated with PT EoS.[3]

and independent errors, having taken into account that the mole fraction is a function of the pump's flow rate and of the densities of the compounds studied

$$x_j = x_j(f_i, \rho_i) \rightarrow u(x_j) = \sqrt{\sum_{i=1}^{2}\left(\frac{\partial x_j}{\partial f_i}\delta f_i\right)^2 + \sum_{i=1}^{2}\left(\frac{\partial x_j}{\partial \rho_i}\delta \rho_i\right)^2} \quad (1)$$

where x_j is the mole fraction of component j, f_i is the flow rate used for component i, and ρ_i is the density of component i.

For the mixture studied in this work, a mean value for the uncertainty in the mole fraction, $u(x_j) = \pm 0.0015$ has been obtained.

Critical Properties. The apparatus has been designed by ARMINES at the École Nationale Supérieure des Mines de Paris (France) and built by TOP-INDUSTRIE. It was designed for measurements of critical properties (P_c and T_c) of pure compounds or mixtures up to 700 K and 20 MPa, by observing the critical opalescence in a sapphire transparent cell. A schematic diagram is shown in Figure 1a. The experimental setup comprises units for loading and measurement.

The measuring section includes a transparent cell (a sapphire tube pressed between two titanium flanges) placed in an air thermostatic bath. The internal volume of the cell is approximately 4 cm^3. The design of the cell and the choice of material take into account the pressure and temperature measurement ranges. The cell temperature is measured using a calibrated 100 Ohm platinum probe centered in the cell with a precision of ±0.03 K. Pressures are measured with a pressure calibrator (Druck Model DPI 145) that is kept at constant temperature by means of a heating cartridge inserted in a brass oven. The pressure calibrator was calibrated by Druck (part of GE Sensing) against a standard secondary pressure transducer, and it has a precision of 0.025% FS.

The uncertainties obtained[14] in the critical temperature and the critical pressure for pure compounds are: repeatability in the critical temperature, $r_{T_c} \leq 0.14$ K, repeatability in the critical pressure, $r_{P_c} \leq 0.011$ MPa, and the confidence intervals, c.i., are c.i.(T_c) < 0.1 K, and c.i.(P_c) < 0.01 MPa. For the mixtures, repeatability in critical temperature and pressure are $r_{T_c} \leq 0.15$ K and $r_{P_c} \leq 0.013$ MPa and the confidence intervals calculated are c.i.(T_c) < 0.32 K and *c.i.*(P_c) < 0.034 MPa.

Densities. Density measurements of pure carbon dioxide and pure propane and of fifteen $\{CO_2(1) + C_3H_8(2)\}$ binary mixtures at 308.15 K and pressures up to 20 MPa were carried out (Figure 1b) using an Anton Paar DMA 512-P vibrating tube densimeter. Temperature is regulated by circulating water from an external temperature controlled circulating bath (Neslab RTE-210) through the heat exchanger of the vibrating tube cell. The temperature is measured with a thermometer (Anton Paar model CKT-100), calibrated with a precision of ±0.01 K. Pressure was determined with a transducer (Druck DPI 145), and it has a precision of 0.025% FS. Finally, a pump (Leybold model D4B) is used for the evacuation and the cleaning of the apparatus. The binary mixtures are generated and homogenized into a third ISCO pump included in the loading unit of the installation.

The model of calibration used in this work is the forced path mechanical calibration model, FPMC, developed by Bouchot and Richon.[15] This includes realistic mechanical considerations and forces representing the stress and strain behavior of the tube material. In the model, the reference fluid is used to find pressure and temperature dependence constants. The reference fluid was water Milli-Q (18.2 mS/cm). The reference densities were calculated using the reference EoS from Wagner and Pruss.[16] The mean relative standard deviation of density, $\bar{s}_\rho^r$ was estimated to be better than 0.1%.[14]

Results

Critical Locus. The experimental results obtained for critical locus of $\{CO_2(1) + C_3H_8(2)\}$ system are collected in Table 1. The P_c-T_c, P_c-x_1 and T_c-x_1 projections of our ($T_c(x)$, $P_c(x)$) measurements are represented in Figures 2 and 3. In these figures, experimental critical locus from the literature,[5–10] and those calculated with the PC-SAFT EoS and PT EoS are also represented. In Figures 2 and 3, after comparing our experimental values for critical locus, which show an "S" shaped representation, with those found in the literature it can be seen that the best agreement is obtained with the values from Horstmann et al.[10] The experimental values for critical locus given by the rest of authors are more scattered than our experimental values and those from Horstmann et al.[10]

We have found in the literature[17–19] that the original PC-SAFT EoS provides an accurate representation of volumetric properties and those of vapor−liquid equilibrium but overestimate the values of critical properties. Because of it, we have tried the following two types of calculation:

(A) When calculating the critical properties of $\{CO_2(1) + C_3H_8(2)\}$ with PC-SAFT EoS, we have adjusted the parameters for characterizing the pure components of the system using the experimental values obtained in this work for critical points of pure CO_2 and C_3H_8. Two of these parameters have a geometrical meaning and a third one is related to energy factors. When calculating the volumetric properties of the studied system with PC-SAFT EoS, the original parameters for pure components have been used. The parameters for pure components for calculating critical and volumetric properties with PC-SAFT EoS are presented in Table 2. The classical mixing rules have been used, and the mixing parameter $k_{ij} = 0.09$, has the same value for both sets of parameters.

(B) We have only used a set of parameters for both, critical and volumetric properties. They were the parameters obtained from our experimental values of critical temperature and pressure of pure compounds. Likewise we have adjusted the experimental density values of pure CO_2 and C_3H_8 by a volume shift, Δv, $\Delta v(CO_2) = 0.17 \times 10^{-3}$ $m^3 \cdot kg^{-1}$ and $\Delta v(C_3H_8) = 0.15 \times 10^{-3}$ $m^3 \cdot kg^{-1}$. The mixing parameter used is the same, $k_{ij} = 0.09$.

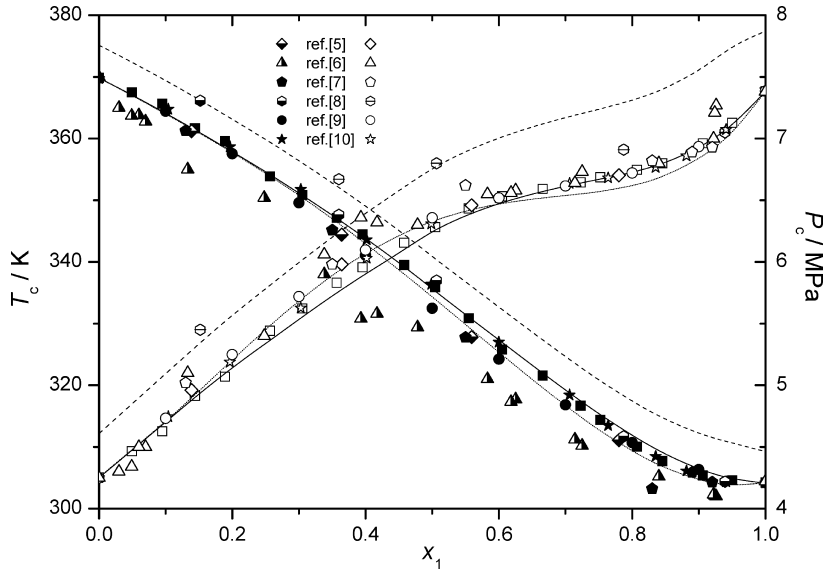

Figure 3. T_c-x_1 and P_c-x_1 planes for the carbon dioxide plus propane system: (■), T_c-x_1 experimental results from this work; (□), P_c-x_1 experimental results from this work; calculated using PC-SAFT EoS[2] with (—) readjusted and (.....) original parameters; (---), calculated with PT EoS.[3]

TABLE 2: Performance of Original and Rescaled Parameters for the PC-SAFT EoS

	original			rescaled		
compound	m	σ (Å)	ε/k (K)	m	σ (Å)	ε/k (K)
CO_2	2.0729	2.7852	169.21	2.1276	2.8251	163.76
C_3H_8	2.0020	3.6184	208.11	2.0577	3.6658	202.42

We have found equivalent results from (A) or (B); the value of the mean relative deviation, MRD (eq 2), obtained from the comparison of our experimental values to those obtained with PC-SAFT (A) or (B) is the same. Therefore we have chosen option (A), as this is the most commonly used to correct the shortcomings of the EoS to predict both critical and volumetric values.

In relation to PT EoS, which has also been used for the theoretical study of $\{CO_2(1) + C_3H_8(2)\}$ system, we have applied the original PT EoS[3] with three parameters and the quadratic mixing rule with $k_{ij} = 0.131$. The values for the MRD, calculated with eq 2, are MRD(P_c) < 0.2% and MRD(T_c) < 1.7% with PC-SAFT EoS and MRD(P_c) < 0.8% and MRD(T_c) < 1.2% with PT EoS.

$$\mathrm{MRD}(\%) = \frac{100}{N}\sum_{n=1}^{N} \left| \frac{x_n^{\exp} - x_n^{\mathrm{cal}}}{x_n^{\exp}} \right| \qquad (2)$$

where N is the number of experimental points and $x = P_c$ or T_c.

The Krichevskii Parameter. The thermodynamic behavior of near-critical dilute solutions is extremely important in understanding the molecular interactions and the microscopic structure of the solutions. In the limit of infinite dilution, many partial molar properties of the solute ($\bar{V}_2^{\infty}$,$\bar{H}_2^{\infty}$,$\bar{C}_{p,2}^{\infty}$) diverge strongly at the solvent's critical point but can be completely characterized by the so-called Krichevskii parameter, $A_{\mathrm{Kr}} = (\partial P/\partial x)^C_{T_c,V_c}$, calculated at the critical point of pure solvent.

The Krichevskii parameter is determined as the slope of the curve of pressure as a function of concentration $P - x$ along the critical isotherm−isochore of pure solvent at $x \to 0$. Krichevskii[20,21] obtained a correlation between the derivative $(\partial P/\partial x)^C_{V_c,T_c}$, the initial slopes of critical lines, $(\partial T_c/\partial x)_{\mathrm{CRL}}$ and $(\partial P_c/\partial x)_{\mathrm{CRL}}$, when $x \to 0$, and the value of the derivative of saturated vapor pressure of pure solvent at the critical point $(\partial P_s/\partial T)^C_{\mathrm{CXC}}$

$$\left(\frac{\partial P}{\partial x}\right)^C_{T_c,V_c} = \left(\frac{\partial P_c}{\partial x}\right)^C_{\mathrm{CRL}} - \left(\frac{\partial P_s}{\partial T}\right)^C_{\mathrm{CXC}}\left(\frac{\partial T_c}{\partial T}\right)^C_{\mathrm{CRL}} \qquad (3)$$

or

$$\left(\frac{\partial P}{\partial x}\right)^C_{T_c,V_c} = \left[\left(\frac{\partial P_c}{\partial T_c}\right)^C_{\mathrm{CRL}} - \left(\frac{\partial P_s}{\partial T}\right)^C_{\mathrm{CXC}}\right]\left(\frac{\partial T_c}{\partial x}\right)^C_{\mathrm{CRL}} \qquad (4)$$

Where $(\partial P_c/\partial T_c)^C_{\mathrm{CRL}}$ and $(\partial T_c/\partial x)^C_{\mathrm{CRL}}$ are the initial slopes of the critical lines (P_c-T_c, T_c-x), and $(\partial P_s/\partial T)^C_{\mathrm{CXC}}$ is the slope of the solvent's vapor pressure curve evaluated at the critical point of the solvent. This quantity is always positive; therefore, in eq 4, the sign of A_{Kr} depends on the correlation between the derivatives $(\partial P_c/\partial T_c)^C_{\mathrm{CRL}}$ and $(\partial P_s/\partial T)^C_{\mathrm{CXC}}$ and on the sign of $(\partial T_c/\partial x)^C_{\mathrm{CRL}}$. For example, in the case of $(\partial P_c/\partial T_c)^C_{\mathrm{CRL}} > (\partial P_s/\partial T)^C_{\mathrm{CXC}}$ for binary mixtures (i.e., the critical line in the T_c-P_c plane lying to the left of the critical T-P isochore of pure solvent), the sign of A_{Kr} coincides with the sign of $(\partial T_c/\partial x)^C_{\mathrm{CRL}}$. Consequently, the shape of the critical lines of this type of mixture at $x \to 0$ (in the vicinity of the CP of pure solvent) fully defines the mode of critical behavior of IDS. We used our experimental data on critical lines to calculate the values of A_{Kr}. The value of the derivative $(\partial P_s/\partial T)^C_{\mathrm{CXC}}$ was determined using the Span and Wagner EoS[22] and the slopes of the critical lines were calculated using the equations as follows:

$$T_c(x) = T_c(CO_2) + \left(\frac{dT_c}{dx}\right)_{x=0} x + Ax^2 + \ldots \qquad (5)$$

$$P_c(x) = P_c(CO_2) + \left(\frac{dP_c}{dx}\right)_{x=0} x + Bx^2 + \ldots \qquad (6)$$

The result is $A_{Kr} = -4.12$ MPa; it can be seen[23] that the agreement with the values from the literature is good, except for those of Furuya and Teja, having taken into account that the error of determination of the proper Krichevskii parameter is 5−10%.

Densities. Measurements of the density of the $\{CO_2(1) + C_3H_8(2)\}$ system as a function of pressure and concentration

TABLE 3: Experimental Density Values, ρ, and Compressibility Factor, Z, for the {CO_2(1) + C_3H_8(2)} Binary System at T = 308.15 K and Several Pressures, P

P/MPa	ρ/ (kg·m^{-3})	Z	P/MPa	ρ/ (kg·m^{-3})	Z	P/MPa	ρ/ (kg·m^{-3})	Z	P/MPa	ρ/ (kg·m^{-3})	Z
					$x_1 = 0.0000$						
0.107	1.64	1.1231	4.997	488.65	0.1760	10.522	503.13	0.3600	15.519	513.81	0.5199
0.531	9.84	0.9289	5.508	490.09	0.1935	11.017	504.26	0.3761	16.018	514.77	0.5356
1.112	23.52	0.8138	6.005	491.53	0.2103	11.529	505.43	0.3926	16.521	515.70	0.5514
1.506	476.92	0.0544	6.512	492.95	0.2274	12.008	506.49	0.4081	17.015	516.62	0.5669
1.998	478.74	0.0718	7.004	494.24	0.2439	12.520	507.61	0.4246	17.508	517.37	0.5825
2.498	480.57	0.0895	7.558	495.62	0.2625	13.017	508.67	0.4405	18.003	518.52	0.5976
2.971	482.22	0.1061	7.988	497.01	0.2767	13.522	509.74	0.4566	18.499	519.45	0.6130
3.487	483.87	0.1240	8.513	498.24	0.2941	14.015	510.78	0.4723	19.039	520.41	0.6297
3.975	485.51	0.1409	9.009	499.51	0.3105	14.528	511.84	0.4886	19.525	521.31	0.6447
4.256	486.39	0.1506	9.503	500.69	0.3267	15.027	512.84	0.5044	19.788	521.83	0.6527
4.480	487.08	0.1583	10.017	501.94	0.3435						
					$x_1 = 0.0501$						
0.108	1.73	1.0745	3.509	498.82	0.1211	6.752	508.56	0.2285	9.001	520.61	0.2976
0.500	9.06	0.9499	4.012	501.24	0.1378	6.999	509.82	0.2363	9.502	522.20	0.3132
1.007	19.57	0.8856	4.509	503.51	0.1541	7.251	510.25	0.2446	9.984	523.76	0.3281
1.923	490.38	0.0675	5.000	505.65	0.1702	7.503	511.23	0.2526	12.960	532.33	0.4190
2.003	490.87	0.0702	5.507	507.84	0.1866	8.005	514.35	0.2679	15.953	539.93	0.5085
2.507	493.67	0.0874	6.001	505.51	0.2043	8.464	518.84	0.2808	20.010	548.96	0.6274
3.013	496.33	0.1045	6.502	507.67	0.2204						
					$x_1 = 0.0998$						
0.108	1.63	1.1403	3.992	502.29	0.1368	6.750	512.75	0.2266	8.95	522.15	0.2950
0.500	8.98	0.9582	4.493	504.62	0.1532	7.007	513.70	0.2347	9.479	523.82	0.3114
1.007	19.38	0.8942	5.006	506.93	0.1699	7.249	514.57	0.2424	9.983	525.50	0.3269
2.507	494.70	0.0872	5.492	509.02	0.1857	7.485	515.45	0.2499	12.996	534.33	0.4186
2.992	497.21	0.1036	6.000	509.81	0.2025	7.978	517.38	0.2654	15.970	541.94	0.5071
3.492	499.82	0.1202	6.493	511.69	0.2184	8.528	520.70	0.2819	19.974	551.24	0.6236
					$x_1 = 0.1508$						
0.108	1.72	1.0805	3.017	500.54	0.1037	6.505	518.72	0.2158	8.963	528.63	0.2918
0.503	9.11	0.9501	3.551	503.79	0.1213	6.994	520.82	0.2311	9.513	530.62	0.3085
1.000	19.53	0.8811	4.101	506.92	0.1392	7.441	522.66	0.2450	9.953	532.15	0.3218
1.510	31.94	0.8135	5.011	511.74	0.1685	7.991	524.86	0.2620	12.95	541.78	0.4113
2.030	160.82	0.2172	5.516	514.19	0.1846	8.502	526.87	0.2777	15.937	549.87	0.4987
2.524	497.47	0.0873	6.013	516.52	0.2003	8.005	518.70	0.2656	19.679	559.25	0.6055
					$x_1 = 0.2500$						
0.109	1.69	1.1096	3.512	508.67	0.1188	6.738	526.94	0.2200	8.993	539.66	0.2867
0.499	8.91	0.9635	4.002	512.39	0.1344	7.011	528.39	0.2283	9.500	541.84	0.3016
1.006	18.95	0.9133	4.490	515.77	0.1498	7.247	529.62	0.2354	10.006	543.95	0.3165
1.503	29.63	0.8727	4.999	519.07	0.1657	7.496	530.73	0.2430	12.982	554.99	0.4024
1.966	67.18	0.5035	5.494	522.07	0.1811	7.994	533.11	0.2580	16.002	564.51	0.4877
2.503	147.78	0.2914	6.013	523.27	0.1977	8.494	537.47	0.2719	19.995	575.52	0.5977
3.010	504.86	0.1026	6.505	525.85	0.2128						
					$x_1 = 0.3230$						
0.108	2.01	0.9243	3.975	515.18	0.1327	7.251	537.31	0.2321	12.000	558.55	0.3696
0.496	9.19	0.9284	5.039	523.11	0.1657	7.508	538.56	0.2398	14.016	565.96	0.4260
1.007	19.45	0.8906	5.884	528.86	0.1914	8.005	540.69	0.2547	15.974	572.41	0.4801
2.045	68.98	0.5100	6.503	532.03	0.2103	9.025	546.18	0.2842	17.925	578.04	0.5334
3.459	418.01	0.1423	6.750	533.12	0.2178	9.904	550.51	0.3095	19.968	584.00	0.5882
3.592	509.21	0.1213	7.024	535.58	0.2256						
					$x_1 = 0.3798$						
0.109	1.73	1.0837	3.992	517.02	0.1328	6.748	537.42	0.2160	8.998	556.00	0.2784
0.500	8.92	0.9641	4.503	522.80	0.1481	7.001	538.10	0.2238	9.499	558.71	0.2924
1.000	18.67	0.9213	4.992	527.69	0.1627	7.247	538.63	0.2314	10.014	561.40	0.3068
1.501	28.68	0.9002	5.506	532.36	0.1779	7.504	539.25	0.2393	12.999	575.02	0.3888
2.004	41.98	0.8211	6.003	536.56	0.1924	7.998	541.00	0.2543	16.000	586.54	0.4692
2.508	95.92	0.4497	6.501	536.99	0.2082	8.482	553.12	0.2638	19.999	599.64	0.5737
3.513	337.18	0.1792									
					$x_1 = 0.4301$						
0.108	2.08	0.8930	4.482	475.84	0.1620	7.253	551.06	0.2264	12.012	578.95	0.3568
0.526	9.80	0.9231	5.000	527.99	0.1629	7.507	551.82	0.2340	14.026	588.35	0.4100
0.968	18.41	0.9043	5.930	537.45	0.1898	8.004	553.62	0.2486	16.039	595.86	0.4629
1.945	47.40	0.7057	6.499	546.57	0.2045	9.032	561.67	0.2766	17.962	602.28	0.5129
3.003	97.35	0.5305	6.749	548.40	0.2117	9.978	568.83	0.3017	19.960	608.48	0.5642
3.794	266.51	0.2448	7.034	550.22	0.2199						
3.814	323.89	0.2025									

TABLE 3: Continued

P/MPa	ρ/ (kg·m^{-3})	*Z*	*P*/MPa	ρ/ (kg·m^{-3})	*Z*	*P*/MPa	ρ/ (kg·m^{-3})	*Z*	*P*/MPa	ρ/ (kg·m^{-3})	*Z*
					$x_1 = 0.5007$						
0.108	1.64	1.1324	3.491	116.65	0.5146	6.755	557.12	0.2085	9.005	574.99	0.2693
0.499	9.23	0.9297	4.001	216.49	0.3178	6.993	560.41	0.2146	9.503	578.75	0.2824
0.998	18.29	0.9383	4.503	347.95	0.2225	7.244	563.52	0.2211	9.993	582.24	0.2951
1.509	28.85	0.8994	4.995	529.16	0.1623	7.482	566.19	0.2272	13.005	600.62	0.3723
2.005	42.71	0.8072	5.485	538.19	0.1753	8.008	569.91	0.2416	16.006	615.22	0.4474
2.496	54.37	0.7894	5.995	546.80	0.1885	8.508	571.03	0.2562	20.011	631.31	0.5451
3.008	66.75	0.7749	6.509	553.75	0.2021						
					$x_1 = 0.5720$						
0.109	1.60	1.1713	4.006	145.02	0.4749	6.752	560.32	0.2072	9.489	588.83	0.2771
0.501	8.72	0.9878	4.116	165.94	0.4265	6.967	561.59	0.2133	9.973	592.99	0.2892
1.003	18.24	0.9454	4.507	213.10	0.3636	7.248	565.91	0.2202	12.030	608.32	0.3400
1.495	28.22	0.9108	4.848	458.64	0.1817	7.501	572.32	0.2253	13.924	622.08	0.3848
2.048	41.65	0.8454	5.067	488.37	0.1784	7.984	574.02	0.2391	16.025	632.93	0.4353
2.511	53.79	0.8026	5.505	535.47	0.1768	8.503	579.49	0.2523	18.022	641.66	0.4829
2.983	65.87	0.7786	5.988	545.69	0.1887	9.001	584.40	0.2648	20.015	649.48	0.5298
3.505	111.03	0.5428	6.502	559.02	0.2000						
					$x_1 = 0.6493$						
0.108	1.69	1.0986	3.508	80.53	0.7488	6.749	559.99	0.2072	9.003	597.40	0.2591
0.496	8.68	0.9823	3.994	135.34	0.5073	7.013	566.41	0.2128	9.517	603.28	0.2712
0.999	18.19	0.9441	5.024	194.28	0.4445	7.253	572.22	0.2179	10.007	608.37	0.2828
1.497	28.24	0.9113	5.511	472.59	0.2005	7.500	576.89	0.2235	12.988	633.41	0.3525
2.009	40.83	0.8458	6.001	534.65	0.1929	7.996	584.79	0.2351	16.011	652.96	0.4215
2.505	55.42	0.7770	6.507	552.83	0.2023	8.483	590.81	0.2468	20.009	673.42	0.5108
3.001	66.18	0.7795									
					$x_1 = 0.6995$						
0.109	1.62	1.1565	4.476	137.30	0.5604	10.029	622.08	0.2771	15.519	672.87	0.3964
0.499	8.54	1.0044	4.963	171.23	0.4982	10.490	629.13	0.2866	15.992	676.04	0.4066
0.998	17.88	0.9594	5.466	194.66	0.4827	11.002	634.95	0.2978	16.504	679.37	0.4176
0.998	17.90	0.9583	6.004	499.08	0.2068	11.497	640.18	0.3087	16.991	682.42	0.4280
1.500	28.85	0.8937	6.485	542.37	0.2055	12.001	645.14	0.3197	17.517	685.61	0.4392
2.000	40.54	0.8480	7.001	563.44	0.2136	12.509	649.79	0.3309	17.992	688.34	0.4493
2.497	51.74	0.8295	7.455	577.10	0.2220	13.024	654.07	0.3423	18.490	691.20	0.4598
2.998	64.71	0.7964	7.984	588.68	0.2331	13.517	658.09	0.3531	19.007	694.05	0.4707
3.503	78.34	0.7686	8.532	599.36	0.2447	13.985	661.78	0.3632	19.472	696.64	0.4804
4.003	93.05	0.7395	9.013	607.42	0.2551	14.582	665.53	0.3766	19.985	699.34	0.4912
4.199	106.08	0.6804	9.558	615.64	0.2669	15.003	669.30	0.3853			
					$x_1 = 0.7611$						
0.108	1.54	1.2053	3.002	64.48	0.8002	6.002	345.80	0.2983	9.005	614.02	0.2521
0.499	8.52	1.0066	3.513	79.06	0.7637	6.502	521.90	0.2141	9.501	622.54	0.2623
0.999	18.00	0.9539	4.015	95.43	0.7231	7.004	556.82	0.2162	9.986	629.89	0.2725
1.498	28.45	0.9049	4.506	112.54	0.6881	7.516	577.84	0.2235	13.000	664.71	0.3361
1.999	40.14	0.8559	5.011	156.53	0.5502	8.013	592.43	0.2325	15.991	689.17	0.3988
2.492	51.22	0.8362	5.486	201.24	0.4685	8.512	604.26	0.2421	19.992	714.22	0.4811
					$x_1 = 0.8499$						
0.108	1.62	1.1456	5.042	130.66	0.6631	7.252	534.45	0.2332	12.034	694.13	0.2979
0.496	9.34	0.9125	6.023	195.53	0.5293	7.501	560.48	0.2300	14.041	718.28	0.3359
1.012	18.95	0.9177	6.379	226.16	0.4847	7.980	577.73	0.2374	16.035	737.29	0.3737
2.008	39.35	0.8769	6.502	284.35	0.3929	9.007	631.01	0.2453	18.031	754.10	0.4109
2.991	62.31	0.8248	7.072	440.32	0.2760	9.738	653.72	0.2560	20.047	767.69	0.4487
4.005	88.56	0.7771									
					$x_1 = 0.8997$						
0.109	1.62	1.1561	3.498	74.67	0.8049	6.411	204.00	0.5400	8.995	636.32	0.2429
0.500	8.58	1.0013	3.999	89.96	0.7638	6.745	270.07	0.4291	9.502	652.62	0.2502
1.000	17.81	0.9647	4.490	105.89	0.7286	7.002	302.05	0.3983	9.992	666.07	0.2578
1.501	27.78	0.9284	5.013	123.91	0.6951	7.266	408.92	0.3053	13.005	720.15	0.3103
2.002	38.14	0.9019	5.519	147.03	0.6449	7.501	517.75	0.2489	16.022	753.86	0.3652
2.498	49.14	0.8734	5.983	174.48	0.5892	8.014	531.24	0.2592	19.995	786.33	0.4369
2.998	61.02	0.8442	6.000	175.45	0.5876	8.509	615.24	0.2376	20.215	788.01	0.4408
					$x_1 = 0.9498$						
0.107	1.77	1.0386	3.498	74.00	0.8121	6.754	213.65	0.5431	9.507	667.43	0.2447
0.500	8.73	0.9840	3.997	87.75	0.7825	7.005	232.54	0.5175	9.990	683.35	0.2512
0.999	17.89	0.9594	4.495	103.76	0.7443	7.244	258.31	0.4818	12.985	745.76	0.2991
1.501	27.69	0.9313	4.996	121.02	0.7092	7.497	284.93	0.4520	15.998	783.25	0.3509
1.999	38.04	0.9028	5.501	141.84	0.6663	8.003	432.60	0.3178	17.014	793.38	0.3684
2.498	49.08	0.8744	6.000	165.94	0.6212	8.506	615.94	0.2373	20.001	818.54	0.4198
3.000	60.85	0.8470	6.509	195.88	0.5709	8.996	645.63	0.2394			

TABLE 3: Continued

P/MPa	ρ/ (kg·m^{-3})	Z	P/MPa	ρ/ (kg·m^{-3})	Z	P/MPa	ρ/ (kg·m^{-3})	Z	P/MPa	ρ/ (kg·m^{-3})	Z
					$x_1 = 1.0000$						
0.107	1.64	1.1208	5.490	136.58	0.6905	10.524	730.59	0.2474	15.531	821.58	0.3247
0.498	8.50	1.0064	5.972	157.30	0.6522	11.019	744.38	0.2543	16.018	827.41	0.3326
1.012	18.00	0.9658	6.500	185.33	0.6025	11.531	756.85	0.2617	16.509	832.72	0.3406
1.499	27.68	0.9303	7.006	220.69	0.5453	12.029	767.76	0.2691	17.041	838.49	0.3491
1.994	37.63	0.9103	7.382	257.76	0.4920	12.523	777.22	0.2768	17.537	843.51	0.3571
2.538	49.66	0.8779	7.525	276.39	0.4677	13.028	786.10	0.2847	18.028	848.24	0.3651
3.019	60.94	0.8510	8.014	429.07	0.3208	13.531	794.37	0.2926	18.527	852.95	0.3731
3.510	73.35	0.8220	8.508	613.13	0.2384	14.022	801.95	0.3004	19.037	857.63	0.3813
4.021	87.16	0.7925	9.023	663.75	0.2335	14.513	808.51	0.3084	19.527	861.77	0.3892
4.527	102.29	0.7603	9.520	692.46	0.2362	15.003	815.00	0.3162	19.928	865.10	0.3957
4.985	117.49	0.7289	10.017	713.47	0.2412						

were performed at 308.15 K for the pure components and for fifteen different concentrations of the mixture. The pressure ranged from 0.1 to 20 MPa. Experimental values for density, ρ, and for the compressibility factor, Z, are presented in Table 3. Some selected experimental results for the mixture are shown in Figures 4−7 along with the values obtained with PC-SAFT and PT EoS. The MRD (eq 2), obtained from the comparison of our experimental values with those obtained with PC-SAFT, is <5% and with PT EoS is <10%.

For mixtures with $x_1 < 0.8454$, a strong change of density is observed, as can be seen in Figure 4, when the sample passes from gaseous to liquid phase. For mixtures with $x_1 > 0.8454$ an inflection point is observed, since the system at these molar fractions and at 308.15 K is a supercritical fluid. Similar results can be observed for the compressibility factor, Z, Figure 5.

As shown in Figure 6, P-ρ plane, the experimental and calculated liquid densities decrease strongly from $x_1 = 1$ to $x_1 = 0$. On the other hand, Figure 7, ρ-x_1 plane, the density−concentration relationship shows almost ideality only at low pressures, but for values bigger than the carbon dioxide's critical pressure ($P_c = 7.383$ MPa), it shows negative deviations from ideality, deviations that increase with pressure.

The values for saturated density, calculated by the tangent method from experimental data, are presented in Table 4 and are represented against the pressure in Figure 8, together with those calculated with PC-SAFT and PT EoS and the data founded in literature.[5] As can be seen in Figure 8, there is good agreement between our data and those calculated with PC-SAFT EoS and data from Niesen.[5] However, the PT-EoS does not provide a good representation of saturated densities for the studied system at 308.15 K.

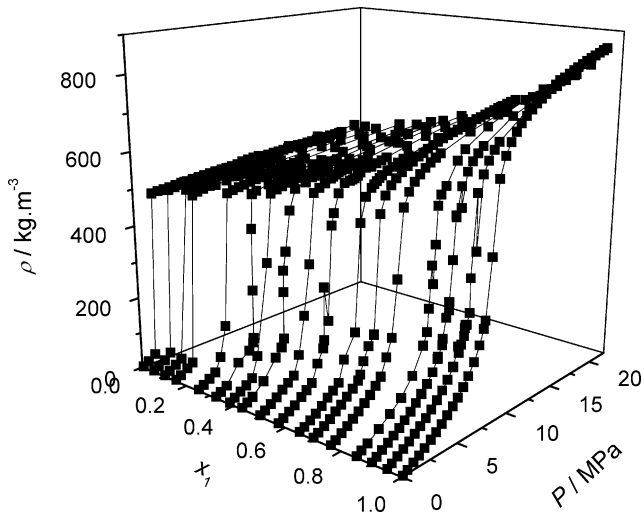

Figure 4. P-x_1-ρ representation of experimental values (■) for {CO_2(1) + C_3H_8(2)} system at $T = 308.15$ K. The solid lines are guides to the eye for better visualization.

Values for V_m^E were calculated from the equation

$$V_m^E = \frac{x_1M_1 + x_2M_2}{\rho} - \frac{x_1M_1}{\rho_1} - \frac{x_2M_2}{\rho_2} \quad (7)$$

where x_1 and x_2 are the molar fractions of carbon dioxide and propane respectively, M_1 and M_2 are their respective molar masses, ρ is the measured density for the mixture at 308.15 K and pressure, P, and ρ_1 and ρ_2 are the measured densities for pure compounds at 308.15 K and pressure, P. The value for the uncertainty of the reported excess molar volumes using the rules of propagation of random and independent errors is ±0.45 cm^3·mol^{-1}.

Some selected values of V_m^E calculated from experimental densities are presented in Table 5 and in Figures 9 and 10. Figure 9 shows our data for V_m^E plotted against pressure, P, for several carbon dioxide molar fractions ($x_1 = 0.0998$, 0.2500, 0.5007, 0.6995, and 0.8997) along with the values obtained with PC-SAFT and PT EoS. Figure 10 shows our data for V_m^E plotted against carbon dioxide molar fraction, x_1, at several pressures ($P = 4$, 7.5, and 20 MPa) together with those obtained with PC-SAFT and PT EoS. As can be observed in these figures, there is good agreement between experimental and calculated values for V_m^E. We are not aware of the existence of previous values of V_m^E for this system in the literature.

It can be observed in Figure 9 that the behavior of V_m^E for the studied mixtures depends strongly on the pressure and the composition, a fact that points to the nonideality of the system. The peak maxima of the V_m^E-P-x_1 curves appear at lower values of pressures and compositions. In the V_m^E-P-x representations, the changes of slope at the right-hand side of the maxima correspond to dew points, while the curve minima are found at the bubble point pressures. The pressures at which these points appear increase as the molar fraction of CO_2 increases.

We can observe three shapes in the representation of V_m^E against x_1 (Figure 10), one for subcritical pressures, such as 4 MPa, a second shape for near-critical pressures, such us 7.5 MPa, and a third one for supercritical pressures, such as 20 MPa.

At 4 MPa and 308.15 K, pure carbon dioxide enters the densimeter as a gas ($\rho = 86.60$ kg·m^{-3}) and pure propane enters as a liquid ($\rho = 485.71$ kg·m^{-3}). For $x_1 < 0.4$, the mixing process consists on the dissolution of gaseous carbon dioxide in liquid propane, and the mixture is a subcritical liquid with a density higher than the value calculated as the weighted mean of the pure component densities; V_m^E is therefore negative. From $x_1 \approx 0.4$ to $x_1 \approx 0.7$, the mixture consists of two phases, and the vapor−liquid ratio increases linearly with the amount of

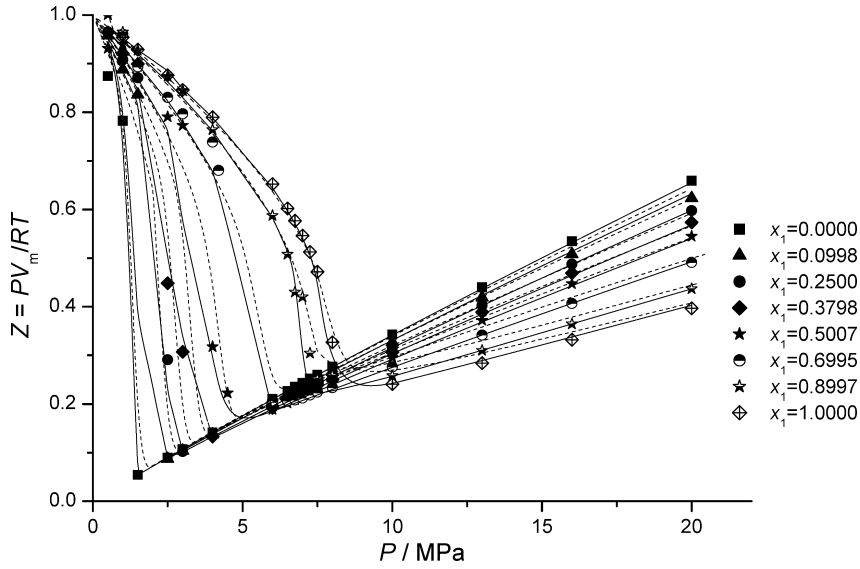

Figure 5. Compressibility factor, Z, of $\{CO_2(1) + C_3H_8(2)\}$ mixture at $T = 308.15$ K as a function of pressure, P, for several compositions, x_1: (symbols), experimental values; (—), calculated using PC-SAFT EoS;[2] (---), calculated with PT EoS.[3]

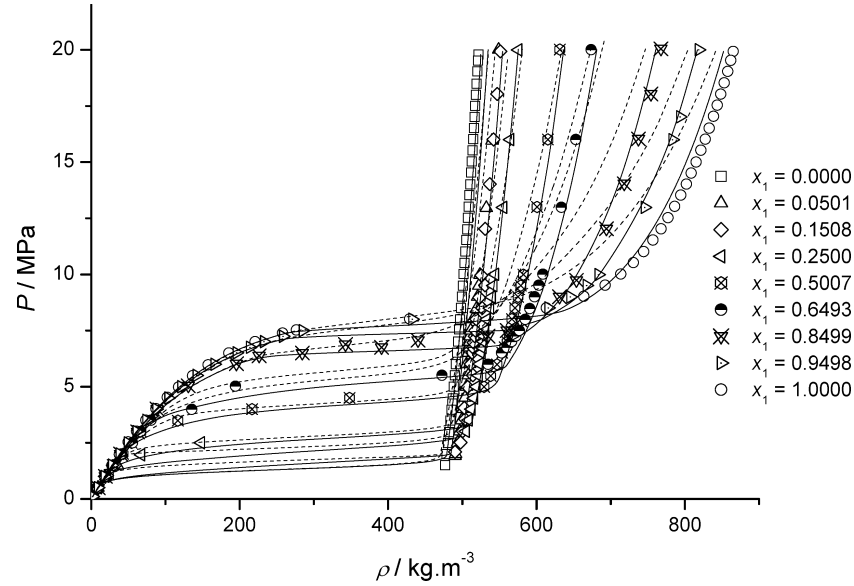

Figure 6. Pressure, P, of $\{CO_2(1) + C_3H_8(2)\}$ mixture at $T = 308.15$ K as a function of density, ρ, for several compositions, x_1: (symbols), experimental values; (—), calculated using PC-SAFT EoS;[2] (---), calculated with PT EoS.[3]

TABLE 4: Saturated Densities Calculated by the Tangent Method for the $\{CO_2(1) + C_3H_8(2)\}$ System

x_1	ρ^v/ kg·m^{-3}	P_{dew}/MPa	ρ^L/ kg·m^{-3}	P_{bubble}/MPa
0.00	23.26	1.112	479.83	1.509
0.05	29.72	1.495	491.07	1.924
0.10	30.62	1.495	498.66	2.518
0.15	31.38	1.510	495.51	2.105
0.25	41.35	2.077	512.53	3.062
0.32	41.96	2.120	519.82	3.560
0.38	62.54	2.780	530.09	4.026
0.43	92.00	3.600	534.25	4.440
0.50	81.06	3.610	545.88	5.384
0.57	94.24	4.110	548.35	5.520
0.65	101.20	4.240	552.25	5.880
0.70	146.20	4.965	554.46	6.420
0.76	170.70	5.380	548.20	6.670
0.85	217.00	6.350	533.20	7.170

carbon dioxide added; the result is a linear variation of the excess volume as x_1 increases. For $x_1 > 0.7$ liquid propane evaporates into the stream of gaseous carbon dioxide, forming a gaseous mixture, and we obtain positive and linearly decreasing V_m^E as the proportion of carbon dioxide in the mixture increases. At 7.5 MPa, near the critical region, carbon dioxide is a gaslike dense fluid ($\rho = 277$ kg·m^{-3}), and propane exhibits a liquidlike density ($\rho = 496$ kg·m^{-3}), but at this pressure and at 308.15 K the mixture never forms two phases for any value of x_1 and crosses the critical locus at $x_1 = 0.9193$. The V_m^E now shows a point of inflection rather than a linear region as shown by the measurements at lower pressures, and the minimum value for the system is nearly -70 cm^3·mol^{-1}. At 20 MPa, pure carbon dioxide is a supercritical fluid (at supercritical temperature and pressure) and pure propane is a liquid, and the mixture formed never crosses the critical locus and never forms two phases. The maximum value of V_m^E for the system studied is near 3 cm^3·mol^{-1}; we have obtained a similar value for this maximum for the $CO_2 + C_2H_6$ system at the same temperature and pressure (in press). These values are much smaller, but still non-negligible, than the values obtained for these systems in the experiments with change of phases, or near the conditions of

dioxide carbon critical point. At 308.15 K and 20 MPa, both systems are always over their critical loci, and the values obtained for the excess volume could be explained by the different densities of the pure compounds ($\rho_{CO_2} = 865.80$ kg·m^{-3}; $\rho_{C_2H_6} = 409.35$ kg·m^{-3}; $\rho_{C_3H_8} = 522.02$ kg·m^{-3}) and the values for the dipole and quadrupole moment of pure compounds. The dipole moments of the pure components are quite similar ($\mu_{CO_2} = 0$ C·m; $\mu_{C_2H_6} = 0$ C·m; $\mu_{C_3H_8} = 0.281 \times 10^{-30}$ C·m),[24] but the quadrupole moments of carbon dioxide, ethane and propane are very different[25–27] ($Q_{CO_2} = -14 \times 10^{-40}$ C·m^2; $Q_{C_2H_6} = -4.3 \times 10^{-40}$ C·m^2; $Q_{C_3H_8} = 1.40 \times 10^{-40}$ C·m^2).

The Krichevskii Function and the Partial Molar Properties. The partial molar volumes, $\bar{V}_i$, with $i = 1, 2$, were obtained from the measured molar volumes V_m using the relations:

$$\bar{V}_1 = V_m - x_2\left(\frac{\partial V_m}{\partial x_2}\right)_{P,T} \quad (8)$$

$$\bar{V}_2 = V_m + (1 - x_2)\left(\frac{\partial V_m}{\partial x_2}\right)_{P,T} \quad (9)$$

The value for the uncertainty of the reported partial molar volumes using the rules of propagation of random and independent errors, is ± 0.15 cm^3·mol^{-1}.

As it is shown in Table 6 and Figure 11a,b, the partial volume, $\bar{V}_1$, decreases as both pressure, P, and carbon dioxide molar fraction, x_1, increase. However, the partial volume, $\bar{V}_2$, Figures 11c,d, slightly decreases with increasing pressure for $0 \le x_1 \le 0.5$; at other compositions $\bar{V}_2$ shows practically no change or perhaps just a slight increase as pressure rises. $\bar{V}_2 - x_1$ isotherms−isobars show a minimum and a maximum, respectively, near $x_1 = 0$ and $x_1 = 1.0$ (dilute mixtures). This behavior is often observed in nonideal mixtures.[28,29]

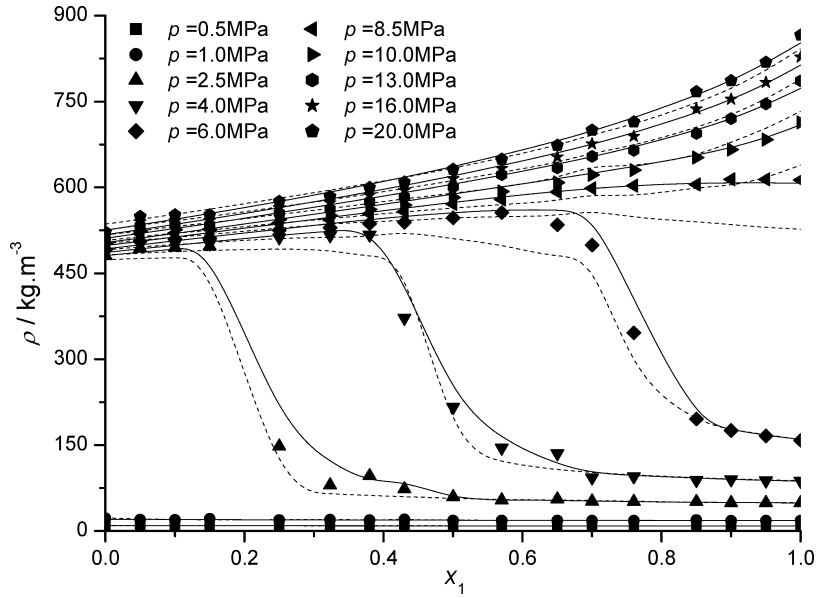

Figure 7. Density, ρ, of $\{CO_2(1) + C_3H_8(2)\}$ mixture at $T = 308.15$ K as a function of composition, x_1, at several pressures, P: (symbols), experimental values; (—), calculated using PC-SAFT EoS;[2] (---), calculated with PT EoS.[3]

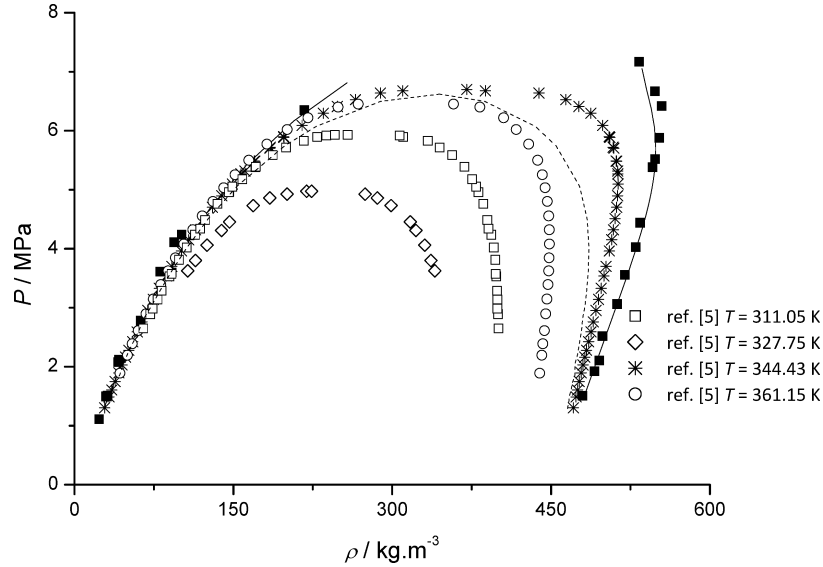

Figure 8. Saturated density behavior of $\{CO_2(1) + C_3H_8(2)\}$ system at $T = 308.15$ K: (■, experimental from this work; (—), calculated using PC-SAFT EoS;[2] (---), calculated with PT EoS.[3]

TABLE 5: Excess Molar Volumes, V_m^E for the {CO_2(1) + C_3H_8(2)} Mixtures at Several Pressures

x_1	V_m^E (cm^3 mol^{-1})	x_1	V_m^E (cm^3 mol^{-1})	x_1	V_m^E (cm^3 mol^{-1})
			P = 4 MPa		
0.0501	–23.71	0.3798	–164.29	0.6995	68.71
0.0998	–44.69	0.4301	–147.35	0.7611	55.99
0.1508	–66.07	0.5007	–96.34	0.8499	51.51
0.2500	–109.13	0.5720	–25.34	0.8997	22.93
0.3230	–140.24	0.6493	54.41	0.9498	12.86
			P = 7 MPa		
0.0501	–8.26	0.3798	–49.21	0.6995	–88.19
0.0998	–14.40	0.4301	–56.53	0.7611	–94.06
0.1508	–20.34	0.5007	–65.81	0.8499	–82.87
0.2500	–33.31	0.5720	–73.81	0.8997	–42.66
0.3230	–42.46	0.6493	–83.00	0.9498	–4.22
			P = 20 MPa		
0.0501	–1.16	0.3798	1.91	0.6995	2.74
0.0998	–0.11	0.4301	2.27	0.7611	2.43
0.1508	0.11	0.5007	2.66	0.8499	1.70
0.2500	0.82	0.5720	2.88	0.8997	1.19
0.3230	1.44	0.6493	2.88	0.9498	0.62

The Krichevskii parameter is described in the critical point, but Japas et al.[30] proposed to extend the use of this derivative to all thermodynamics states since it is such an important parameter in dilute mixtures. Consequently, they denoted $J = (\partial P/\partial x)_{T,V}^{\infty}$ as the Krichevskii function.

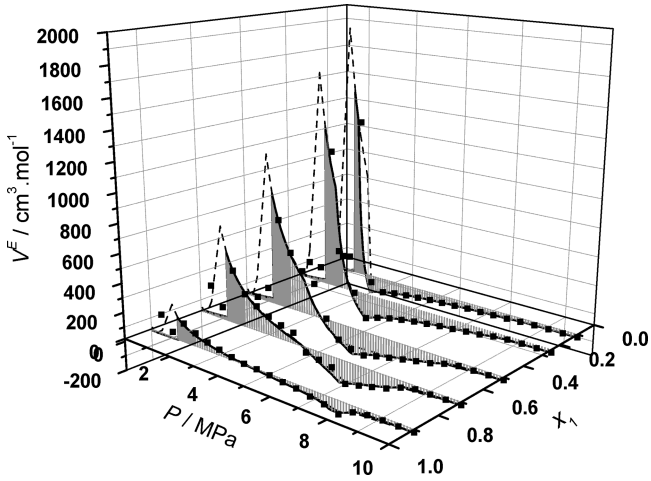

Figure 9. Excess molar volumes, V_m^E for {CO_2(1) + C_3H_8(2)} system as a function of pressure, P, at T = 308.15 K for various compositions, x_1: (symbols), experimental values; (—), calculated using PC-SAFT EoS;[2] (---), calculated with PT EoS.[3]

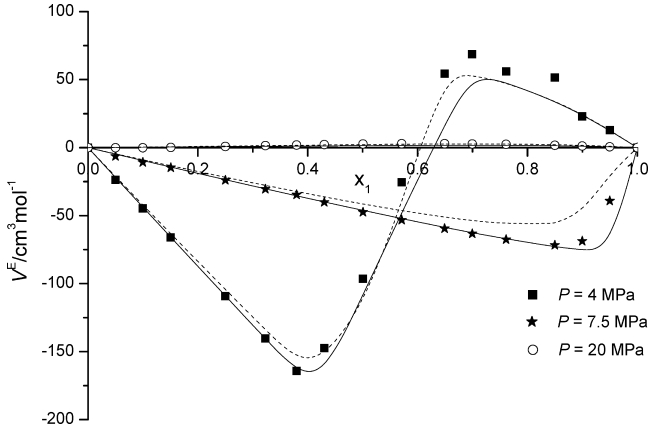

Figure 10. Excess molar volumes, V_m^E for {CO_2(1) + C_3H_8(2)} system as function of composition, x_1, at T = 308.15 K at several pressures, P: (symbols), experimental values; (—), calculated using PC-SAFT EoS;[2] (---), calculated with PT EoS.[3]

For infinite dilute solutions, IDS, the partial molar volume, $\bar{V}_2^{\infty}$, may be expressed in terms of the Krichevskii function, J. $(\partial V_m/\partial x)_{P,T} = -(\partial P/\partial x)_{TV}(\partial V_m/\partial P)_{T,x}$ and at $x \to 0$, $(\partial P/\partial x)_{TV}^{\infty}$ is the Krichevskii function, V_m is V_1 and $(\partial V_1/\partial P)_T$is the isothermal compressibility of pure solvent, k_T.

Therefore,

$$\bar{V}_2^{\infty} = V_1 - \left(\frac{\partial P}{\partial x}\right)_{TV}^{\infty}\left(\frac{\partial V_1}{\partial P}\right)_x = V_1[1 + k_T J] = \rho^{-1}\left[k_T\left(\frac{\partial P}{\partial x}\right)_{TV}^{\infty} + 1\right] \tag{10}$$

where ρ is the density of pure solvent.

In the proximity of the critical point of pure solvent, $x \to 0$, the Krichevskii function, $J = (\partial P/\partial x)_{TV}^{\infty}$ converges to the Krichevskii parameter, A_{Kr}, and $k_T = (\partial V_1/\partial P)_{T,x}$, the compressibility of pure solvent, k_T diverges at the solvent critical point (large scale fluctuations of the order parameter). Therefore the partial molar volume, $\bar{V}_2^{\infty}$, of the solute will be a diverging function as well. In the proximity to the critical point of pure solvent, $T \to T_C$, $k_T \propto (T - T_C)^{-\gamma} \to \infty$, therefore $\bar{V}_2^{\infty} \to \pm\infty$, the sign depends on the sign of the Krichevskii parameter, and the Krichevskii parameter defines the sign of divergence of the partial molar volume $\bar{V}_2^{\infty}$. The value of A_{Kr} calculated by us is −4.12 MPa, so for the CO_2(1) + C_3H_8(2) system at the critical temperature of CO_2, $\bar{V}_2^{\infty} \to -\infty$. On approaching the critical point of pure solvent $T \to T_C$, the slope of $(\partial V_m/\partial x)_{P,T}^{\infty}$ increases infinitely, and as a consequence, the value of derivative $(\partial V_m/\partial x)_{P,T}^{\infty}$ prevails in the calculation of the partial molar volume. Given that experimental values for density in this work at 308.15 K and that the studied mixtures cannot be considered as infinitely dilute solutions, no values for $\bar{V}_2^{\infty}$ were obtained. Nevertheless, we calculated values for $\bar{V}_2^{\infty}$ with PC-SAFT EoS, and we found a diverging function with a minimum value of ≈ -2500 cm^3·mol^{-1} at the critical density of carbon dioxide.

Structural Properties. The Krichevskii function was calculated from an adjusted function of our experimental data, $P = P(\rho, x)$ for {CO_2(1) + C_3H_8(2)} mixtures. The calculated values of the Krichevskii function as a function of density, along with the values obtained with PC-SAFT and PT EoS, are shown in Figure 12.

In this section, we study the ideality of the mixtures using the Krichevskii function concept from the viewpoint of structural

TABLE 6: Partial Molar Volumes, $\bar{V}_i$, for {CO_2(1) + C_3H_8(2)} Mixtures at Several Pressures

x_1	$\bar{V}_1$ (cm^3 mol^{-1})	$\bar{V}_2$ (cm^3 mol^{-1})	x_1	$\bar{V}_1$ (cm^3 mol^{-1})	$\bar{V}_2$ (cm^3 mol^{-1})
		$P = 10$ MPa			
0.0000	69.741	87.859	0.5720	63.850	88.108
0.0501	66.428	85.085	0.6493	63.601	88.720
0.0998	66.548	85.743	0.6995	63.102	88.760
0.1508	67.041	86.775	0.7611	63.578	89.883
0.2500	65.424	86.235	0.8499	63.430	90.704
0.3230	65.362	86.959	0.8997	63.306	91.119
0.3798	64.722	86.933	0.9498	62.992	91.344
0.4301	64.469	87.219	1.0000	61.684	90.574
0.5007	63.913	87.417			
		$P = 13$ MPa			
0.0000	68.435	86.697	0.5720	58.197	87.527
0.0501	64.564	83.797	0.6493	58.657	89.540
0.0998	64.333	84.537	0.6995	57.771	89.626
0.1508	64.560	85.735	0.7611	58.317	91.337
0.2500	62.082	85.198	0.8499	58.207	92.975
0.3230	61.808	86.343	0.8997	57.551	93.289
0.3798	60.736	86.377	0.9498	57.165	93.874
0.4301	60.408	87.020	1.0000	55.985	93.665
0.5007	59.364	87.335			
		$P = 16$ MPa			
0.0000	67.009	85.669	0.5720	55.993	87.626
0.0501	62.861	82.659	0.6493	55.736	89.190
0.0998	62.506	83.442	0.6995	54.762	89.354
0.1508	62.554	84.628	0.7611	55.261	91.219
0.2500	59.818	84.168	0.8499	54.032	92.038
0.3230	59.303	85.314	0.8997	54.466	93.610
0.3798	58.197	85.506	0.9498	54.181	94.463
0.4301	57.838	86.285	1.0000	53.190	94.610
0.5007	56.589	86.629			
		$P = 20$ MPa			
0.0000	64.860	84.483	0.5720	53.715	86.638
0.0501	60.575	81.365	0.6493	53.223	88.013
0.0998	60.114	82.071	0.6995	52.123	88.080
0.1508	60.212	83.335	0.7611	52.688	90.045
0.2500	57.510	82.966	0.8499	51.478	90.935
0.3230	57.077	84.237	0.8997	51.918	92.542
0.3798	55.823	84.313	0.9498	51.682	93.473
0.4301	55.446	85.103	1.0000	50.820	93.777
0.5007	54.138	85.428			

and thermodynamic properties. This quantity is related to total (TCFI) and direct (DCFI) correlation function integrals[4,31–38] and summarizes the effects of the intermolecular interactions between solvent and solute particles which affect the properties of the solution.

$$J = \frac{\rho_1(H_{11} - H_{12})}{k_T} \tag{11}$$

$$J = RT\rho_1^2(C_{11} - C_{12}) \tag{12}$$

where H_{11} and H_{12} are the TCFI defined as $H_{ij} = \int h_{ij}(r)\mathrm{d}r$; $h_{ij}(r) = g_{ij}(r) - 1$ is the total correlation function for *i-j* pair interactions, $g_{ij}(r)$ is the pair correlated function, sometimes called the radial distribution function. The magnitude of $g_{ij}(r)$ represents the probability of finding a particle *i* at a distance *r* from a particle *j* in relation to the bulk average. $H_{11} = (k_T RT) - \rho_1^{-1}$ is the TCFI for *i-i* (pure solvent molecules) pair interactions. C_{11} and C_{12} are the DCFI defined as $C_{ij} = \int c_{ij}(r)\mathrm{d}r$; $c_{ij}(r)$ is the direct correlation function for *i-j* pair interactions, and $(1 - \rho_1 C_{11}) = (\rho_1 k_T RT)^{-1}$ is the DCFI for *i-i* (pure solvent molecules) pair interactions.

As eqs 11 and 12 show, the Krichevskii function, *J*, expresses the difference between solvent−solute (1-2) and solvent−solvent (1-1) interactions, therefore it gives a representation of the ideality of the mixture. If $(C_{11} - C_{12})$ and $(H_{11} - H_{12})$ are very small or zero, *J* will also be very small or zero, which means that the interactions between different types of molecules are similar. Negative values for the Krichevskii function, as those obtained in this work (see Figure 12), mean that the interaction between carbon dioxide and propane molecules is attractive. The Krichevskii function has also a physical meaning, given that its value accounts for the variation of the pressure in the system when one molecule of solvent is replaced by a molecule of solute at constant values of *T* and *V*.

The values obtained in this work for C_{ii}, C_{ij}, H_{ii}, and H_{ij} show that the differences $(C_{11} - C_{12})$ and $(H_{11} - H_{12})$ are not small (Figures 13−15). Therefore, from a microscopic viewpoint, the dilute carbon dioxide and propane mixture is not ideal. The nonideality of the studied system was shown above, when discussing the values of the measured and derived volumetric properties. At 308.15 K and pressures from 7.5 to 9.0 MPa, the density of CO_2 ranged from 277 kg·m^{-3} to 660 kg·m^{-3}, the system is over its critical locus, the excess molar volumes are negative and the values of *J* are not small negative amounts; the negative values of the Krichevskii function mean that the interaction between carbon dioxide and propane molecules is attractive. From pressure values slightly smaller than 10 MPa, the excess molar volumes become positive, which is consistent

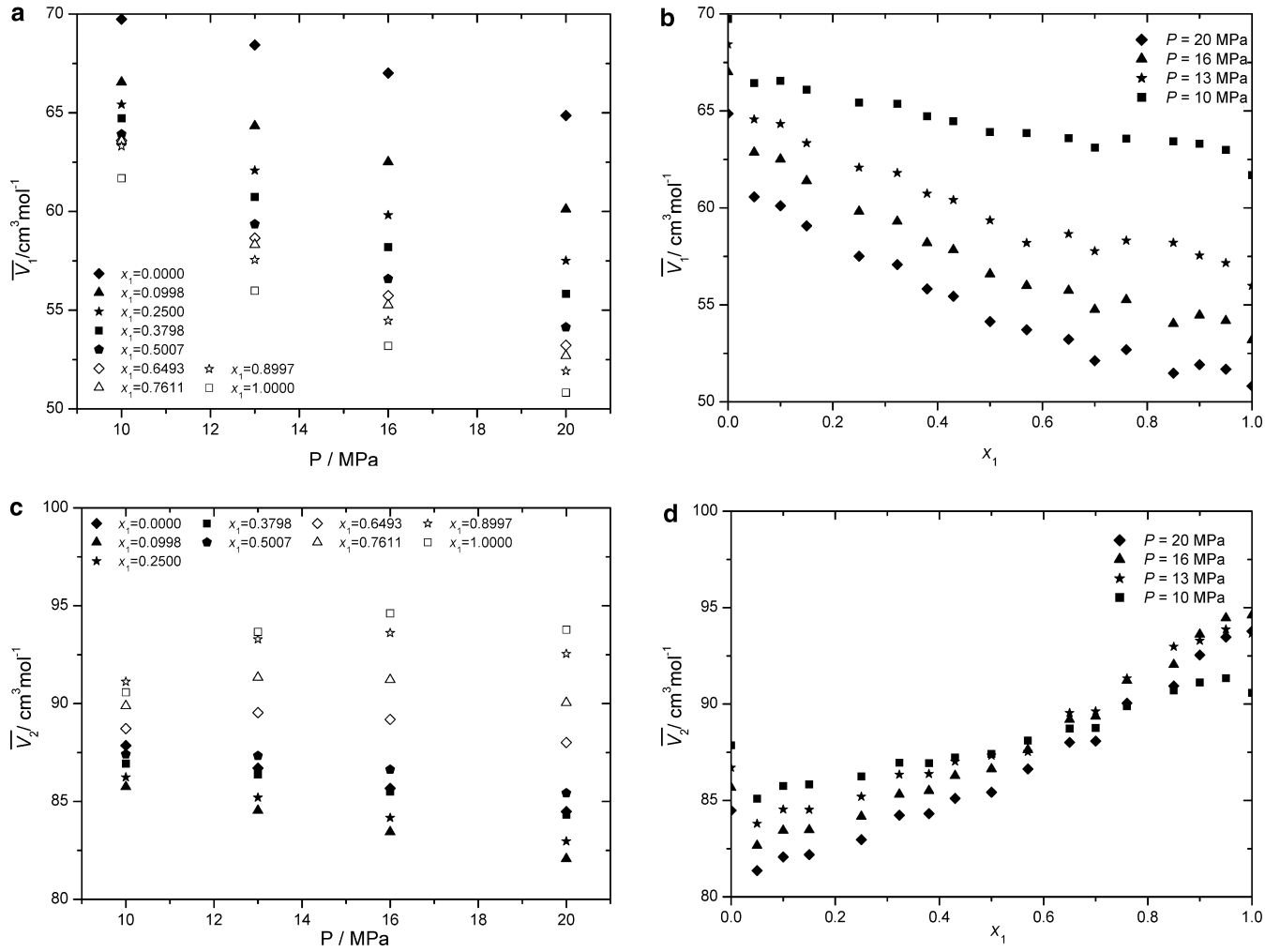

Figure 11. (a,c) Partial molar volumes, $\bar{V}_i$ (i = 1, 2), for {CO_2(1) + C_3H_8(2)} system as function of pressure, P, at T = 308.15 K for several compositions, x_1; (b,d) Partial molar volumes $\bar{V}_i$ (i = 1, 2), for {CO_2(1) + C_3H_8(2)} system as function of composition, x_1, at T = 308.15 K at several pressures, P. (Symbols), experimental values.

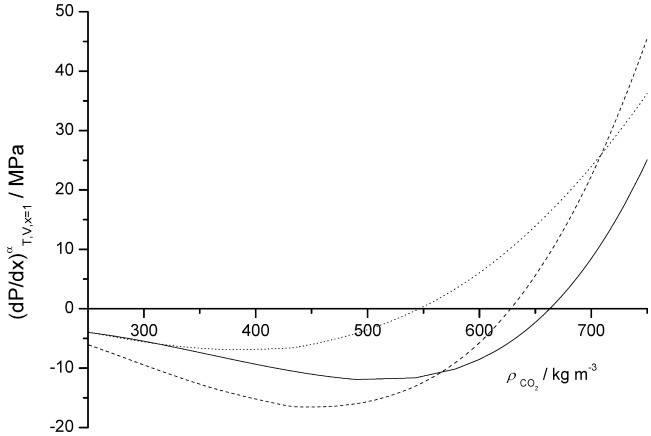

Figure 12. Plot of the Krichevskii function, J, against density of the pure solvent (CO_2), for the {CO_2(1) + C_3H_8(2)} mixture at T = 308.15 K calculated: (—), from our experimental data; (.....), using PC-SAFT EoS;[2] (---), with PT EoS.[3]

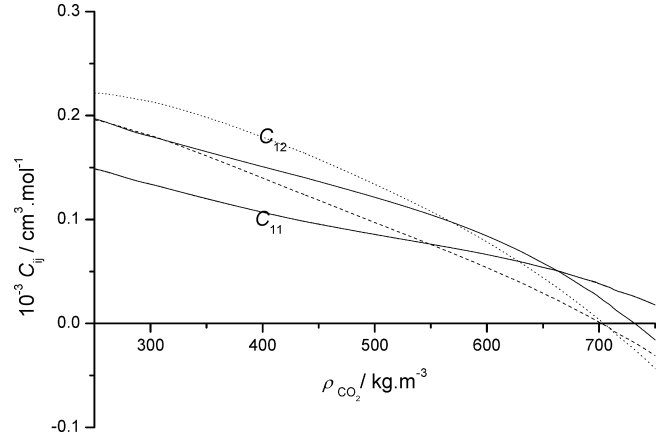

Figure 13. Direct correlation function integrals, C_{ij}, against density of the pure solvent (CO_2) for the {CO_2(1) + C_3H_8(2)} mixture at T = 308.15 K calculated: (—), from our experimental data; (.....), using PC-SAFT EoS;[2] (---), with PT EoS.[3]

with values of J higher than zero for densities of carbon dioxide bigger than approximately 660 kg·m^{-3} (Figure 12).

Another verification of the microscopic behavior of the mixture is the value obtained for the microstructural parameter, N^{∞}_{exc}, which is defined as the excess number (or excess coordination number), $N^{\infty}_{exc} = (N_{12} - N_{11})$, where N_{12} indicates that each propane molecule is surrounded by a cage of N_{12} molecules of carbon dioxide, while each CO_2 molecule in the bulk is surrounded by a cage of N_{11} CO_2 molecules. The microscopic definition of the excess coordination number is $N^{\infty}_{exc} = 4\pi\rho\int_0^{R_{shell}}[g_{12}(r) - g_{11}(r)]\, r^2\, dr$, where $g_{12}(r)$ and $g_{11}(r)$ are the radial distribution functions for the solvent−solvent (1-1) and solvent−solute (1-2) interactions, respectively.

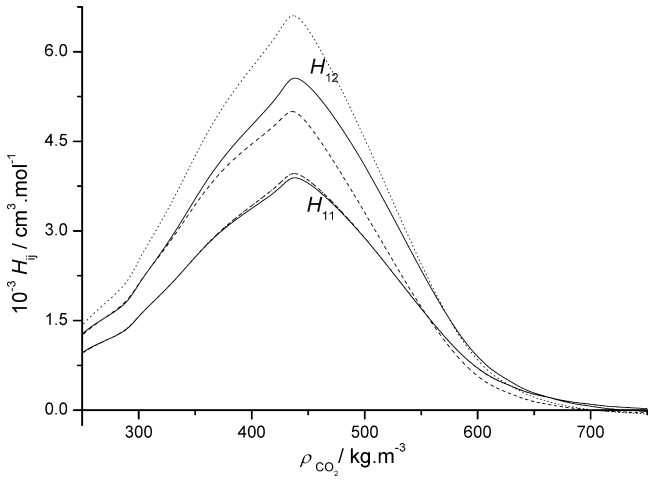

Figure 14. Total correlation function integrals, H_{ij}, against density of the pure solvent (CO_2) for the $\{CO_2(1) + C_3H_8(2)\}$ mixture at $T = 308.15$ K calculated: (—), from our experimental data; (.....), using PC-SAFT EoS;[2] (---), with PT EoS.[3]

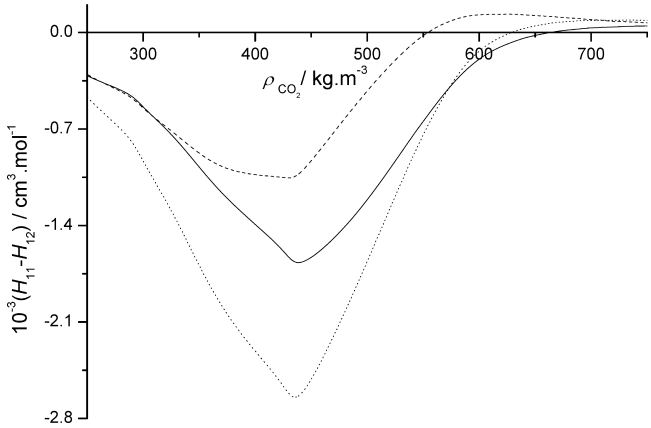

Figure 15. Total correlation function integrals differences for 1-1 and 1-2 pair interaction between CO_2-CO_2 and $CO_2-C_3H_8$ against density of the pure solvent (CO_2) for the $\{CO_2(1) + C_3H_8(2)\}$ mixture at $T = 308.15$ K calculated: (—), from our experimental data; (.....), using PC-SAFT EoS;[2] (---), with PT EoS.[3]

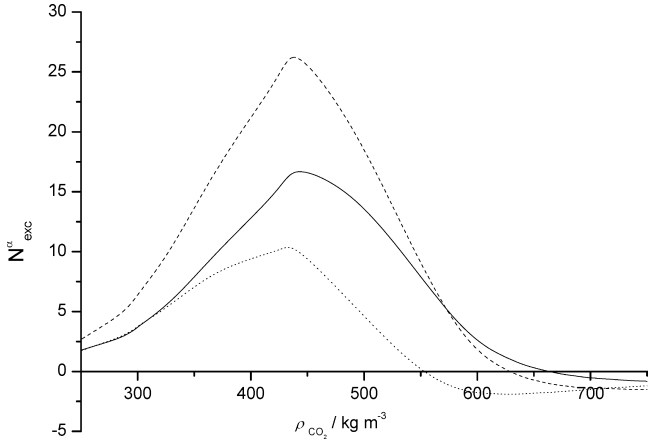

Figure 16. Excess coordination number (cluster size, N^{∞}_{exc}) around a propane molecule against density of the pure solvent (CO_2), for the $\{CO_2(1) + C_3H_8(2)\}$ mixture at $T = 308.15$ K calculated: (—), from our experimental data; (. ....), using PC-SAFT EoS [2]; (---), with PT EoS [3].

The values of N^{∞}_{exc} are also related to the Krichevskii function as follows:

$$N^{\infty}_{exc} = -k_T\left(\frac{\partial P}{\partial x}\right)^{\infty}_{T,V} \quad (13)$$

Thus, the Krichevskii function also defines the microscopic phenomena involving local density perturbations induced by the presence of the solute molecules. Therefore, J measures the finite microscopic rearrangement of the solvent structure around the infinitely dilute solute relative to the solvent structure ideal mixture. In Figure 16, the values of N^{∞}_{exc} calculated with eq 13 are shown.

As it can be seen in Figure 16, the excess number of solvent molecules, N^{∞}_{exc}, around the solute molecules is not nearly zero, $N_{12} \neq N_{11}$, especially in the proximity of critical density of dioxide carbon. This means that when exchanging a solvent molecule (carbon dioxide) for one solute molecule (propane), at constant volume and temperature, the local density (coordination number) of carbon dioxide molecules around propane molecules is higher than in the ideal mixture (local environmental around infinitely dilute propane is higher than the bulk density of pure carbon dioxide).

Debenedetti[35] stated that IDS in the vicinity of a solvent's critical point exhibit one of three types of behavior: repulsive, weakly attractive, or attractive. Each regime is characterized by the signs of the diverging solute partial molar volume and of the correlations between solute and solvent concentration fluctuations at infinite dilution. In relation to attractive behavior, in which the former quantity is negative and the latter is positive, the presence of trace amounts of a solute within a solvent characterized by long-ranged density fluctuations gives rise to a cooperative phenomenon that involves the formation of a large solvent-rich region around each solute molecule.

Our system exhibits a negative value for the Krichevskii function, $J < 0$, $\bar{V}_2^{\infty} \rightarrow -\infty$ and $N^{\infty}_{exc} \rightarrow +\infty$ when conditions characterizing the critical point of the solvent arise. Typically attractive behavior is volumetric collapse upon addition of solute and large excess number buildup.

Conclusions

The critical locus (P_c, T_c, x_c) of binary $\{CO_2(1) + C_3H_8(2)\}$ system has been measured in addition to the densities of 15 concentrations of the mixture at $T = 308.15$ K and pressures ranging from 0.1 to 20 MPa. Measurements were carried out with an experimental setup that includes a flow apparatus for critical temperature and pressure (P_c, T_c) determination, using a critical opalescence method, and a vibrating-tube densimeter for the measurement of volumetric properties (P-ρ-T).

Other properties related with P-ρ-T-x data such as compressibility factor, Z, excess molar volumes, V^E_m, and partial molar volumes, $\bar{V}_i$, have been calculated from densities measured as a function of pressure and concentration. Additionally, the derived values of saturated density calculated by the tangent method are also presented.

Both the critical and volumetric behavior have been compared with literature data and values obtained from the PC-SAFT and PT EoS. The mean relative deviation, MRD, obtained from the comparison of our experimental values for critical properties with those obtained with PC-SAFT EoS is MRD(P_c) < 0.2% and MRD(T_c) < 1.7%; MRD(P_c) < 0.8% and MRD(T_c) < 1.2% when using PT EoS. The deviations obtained in the calculation of densities with PC-SAFT EoS in comparison to experimental values is MRD < 5%, and with PT EoS MRD < 10%.

The data on critical line of the system studied was used to determine the value of the Krichevskii parameter, $A_{Kr} = -4.12$ MPa, which is in good agreement with the literature. Furthermore, the Krichevskii function was calculated using an adjusted

function from the experimental values in this work, $P = P(\rho, x)$ for dioxide carbon plus propane mixtures. The values for this function and for the properties of pure CO_2 in the vicinity of the critical point were used to calculate the structural properties (direct and total correlation function integrals, size of cluster) of IDS of $\{CO_2(1) + C_3H_8(2)\}$ in the vicinity of the critical point of pure CO_2. The sign of Krichevskii function, negative, indicates a typically attractive behavior for the dilute mixture near the conditions of the critical point of solvent: volumetric collapse upon addition of solute and large excess number buildup.

The values obtained for the structural properties, from the microscopic viewpoint, show that the dilute carbon dioxide plus propane mixture is not ideal. The nonideality of the studied system is also shown by the values obtained in this work for the experimental and derived volumetric properties.

In this work, the computations of the different properties were performed using the phase Equilibria software (PE 2000, version 2.9.9b) for the PT[39] and the VLXE software for the PC-SAFT EoS[40] calculations.

Acknowledgment. The authors gratefully acknowledge the financial support received from Gobierno de Aragón DGA (005/2000), Ministerio de Educación y Ciencia of Spain (BQU 2001-2514, FIS 2004-02180, CTQ 2005-02213), and Universidad de Zaragoza (INF2004-CIE-23, INF2005-CIE-006).

List of Symbols

T = temperature
P = pressure
V = volume
x = mole fraction
u = uncertainty
r = repeatability
c.i. = confidence interval
$\overline{s}^r$ = mean relative standard deviation
MRD = mean relative deviation
f = flow rate
Z = compressibility factor
V_m^E = excess molar volumes
$\bar{V}$ = partial molar volumes
Q = quadrupole moment
k = binary interaction parameter
A_{Kr} = Krichevskii parameter
J = Krichevskii function
k_T = isothermal compressibility
R = universal gas constant
g = radial distribution function
C = direct correlation function integral
H = total correlation function integral
N_{exc} = excess coordination number

Greek Letters

ρ = density
μ = dipole moment

Subscripts

c = critical property
s = saturated property
i,j = components
1,2 = components

Superscripts

L = liquid phase
V = vapor phase
∞ = infinite dilution

References and Notes

(1) Seevam, P. N.; Hopkins, P.; Race, J. M.; Downie, M. J. International Conference on Petroleum Sustainable Development2007, Beijing China.
(2) Gross, J.; Sadowski, G. *Ind. Eng. Chem. Res.* **2001**, *40*, 1244.
(3) Patel, N. C.; Teja, A. S. *Chem. Eng. Sci.* **1982**, *37*, 463.
(4) Levelt Sengers, J. M. H. *J. Supercrit. Fluids* **1991**, *4*, 215.
(5) Niesen, V. G.; Rainwater, J. C. *J. Chem. Thermodyn.* **1990**, *22*, 777.
(6) Martin, A.; Mothes, S.; Mannsfeld, G. *Fresenius' J. Anal. Chem* **1999**, 364.
(7) Roof, J. G.; Baron, J. D. *J. Chem. Eng. Data* **1967**, *12*, 292.
(8) Poettmann, F. H.; Katz, D. L. *Ind. Eng. Chem.* **1945**, *37*, 847.
(9) Van Poolen, L. J.; Holcomb, C. D. *Fluid Phase Equilib.* **1999**, *165*, 157.
(10) Horstmann, S.; Fischer, K.; Gmehling, J. *Chem. Eng. Technol.* **1999**, *22*, 839.
(11) Reamer, H. H.; Sage, B. H.; Lacey, W. N. *Ind. Eng. Chem.* **1951**, *43*, 2515.
(12) Galicia Luna, L. A.; Richon, D.; Renon, H. *J. Chem. Eng. Data* **1994**, *39*, 424.
(13) de la Cruz de Dios, J.; Bouchot, C.; Galicia Luna, L. A. *Fluid Phase Equilib.* **2003**, *210*, 175.
(14) Gil, L.; Otín, S.; Muñoz Embid, J.; Gallardo, A.; Blanco, S.; Artal, M.; Velasco, I. *J. Supercrit. Fluids* **2008**, *44*, 123.
(15) Bouchot, C.; Richon, D. *Fluid Phase Equilib.* **2001**, *191*, 189.
(16) Wagner, W.; Pruss, A. *J. Phys. Chem. Ref. Data* **2002**, *31*, 387.
(17) Cismondi, M.; Brignole, E. A.; Mollerup, J. *Fluid Phase Equilib.* **2005**, *234*, 108.
(18) Alfradique, M. F.; Castier, M. *Fluid Phase Equilib.* **2007**, *257*, 78.
(19) Arce, P.; Aznar, M. *J. Supercrit. Fluids* **2007**, *42*, 1.
(20) Krichevskii, I. R. *Zh. Fiz. Khim.* **1967**, *41*, 2458.
(21) Rozen, A. M. *Zh. Fiz. Khim.* **1976**, *50*, 1381.
(22) Span, R.; Wagner, W. *J. Phys. Chem. Ref. Data* **1996**, *25*, 1509.
(23) Abdulagatov, A. I.; Stepanov, G. V.; Abdulagatov, I. M. *High Temp.* **2007**, *45*, 408.
(24) *Selected values of electric dipole moments for molecules in the gas phase*; Nelsonr, R. D., Jr., Lide, D. R., Jr., Maryott, A. A., Eds.; National Reference Data Series - NBS 10; **1967**.
(25) Reynolds, L.; Gardecki, J. A.; Frankland, S. J. V.; Horng, M. L.; Maroncelli, M. *J. Phys. Chem.* **1996**, *100*, 10337.
(26) Amos, R. D.; Williams, J. H. *Chem. Phys. Lett.* **1979**, *66*, 471.
(27) Merz, R.; Linder, F. *J. Phys. B: At. Mol. Opt. Phys.* **2003**, *36*, 2921.
(28) Kubota, H.; Tanaka, Y.; Makita, T. *Int. J. Thermophys* **1987**, *8*, 47.
(29) Abdulagatov, J. M.; Tekin, A.; Safarov, J.; Shahverdiyev, A.; Hassel, E. *J. Chem. Thermodyn.* **2008**, *40*, 1386.
(30) Japas, M. L.; Alvarez, J. L.; Gutkowski, K.; Fernandez-Prini, R. *J. Chem. Thermodyn.* **1998**, *30*, 1603.
(31) Levelt Sengers, J. M. H.; Morrison, G.; Nielson, G.; Chang, R. F.; Everhart, C. M. *Int. J. Thermophys.* **1986**, *7*, 231.
(32) Fernandez-Prini, R.; Japas, M. L. *Chem. Soc. Rev.* **1994**, *23*, 155.
(33) Chang, R. F.; Levelt Sengers, J. M. H. *J. Phys. Chem.* **1986**, *90*, 5921.
(34) Chialvo, A. A.; Cummings, P. T. *AIChE J.* **1994**, *40*, 1558.
(35) Debenedetti, P. G.; Mohamed, R. S. *J. Chem. Phys.* **1989**, *90*, 4528.
(36) McGuigan, D. B.; Monson, P. A. *Fluid Phase Equilib.* **1990**, *57*, 227.
(37) Brelvi, S. W.; O'Connell, J. P. *AIChE J.* **1972**, *18*, 1239.
(38) O'Connell, J. P. *Mol. Phys.* **1971**, *20*, 27.
(39) Pfohl, O.; Petkov, S.; Brunner. G. *Usage of PE - A program to calculate Phase Equilibria*, English Software Manual; Utz-Verlag: München, Germany, 1998; ISBN: 3-89675-410-6.
(40) Laursen, T. *VLXE ApS*; Scion-DTU: Diplomvej, Denmark, 2007.

JP9005873